NMR solution structure and position of transportan in neutral phospholipid bicelles

Elsa Bárány-Wallje, August Andersson, Astrid Gräslund, Lena Mäler*

Department of Biochemistry and Biophysics, The Arrhenius Laboratories, Stockholm University, S-10691 Stockholm, Sweden

Abstract Transportan is a chimeric cell-penetrating peptide constructed from the peptides galanin and mastoparan, which has the ability to internalize living cells carrying a hydrophilic load. In this study, we have determined the NMR solution structure and investigated the position of transportan in neutral bicelles. The structure revealed a well-defined -helix in the C-terminal mastoparan part of the peptide and a weaker tendency to form an -helix in the N-terminal domain. The position of the peptide in relation to the membrane, as studied by adding paramagnetic probes, shows that the peptide lies parallel to, and in the head-group region of the membrane surface. This result is supported by amide proton secondary chemical shifts.
© 2004 Federation of European Biochemical Societies. Published by Elsevier B.V. All rights reserved.

Keywords: Cell-penetrating peptide; Transportan; NMR; Solution structure; Bicelle

1. Introduction

It has been discovered that several short peptides, so called cell-penetrating peptides (CPPs), have the capability to transfer large hydrophilic cargos into living cells without destroying the cell. The prospect of using CPPs for delivery of drugs into the cell puts them into focus of intensive research [1,2]. The translocation through the membrane was originally thought not to be dependent on active transport or receptors, but several recent findings have shown that the translocation mechanism may involve different pathways for different peptides and cargoes, as well as in different membrane environments. In recent studies it was shown that fluorescence microscopy on fixed cells, which is a method by which several translocation observations have been made, can give artifactual uptake of peptide associated with the plasma membrane, and that endocytotic pathways may dominate for many systems [3–5]. Other translocation mechanisms have also been proposed [6,7], and since the mechanism of cell internalization is not fully known, further work is needed in order to clarify whether the internalization is dependent on the structure of the peptide or on the orientation of the peptide in relation to the membrane.

Transportan is a 27 residues long peptide with the sequence: GWTLNSAGYLLGKINLKALAALAKKIL-amide. It is a chimeric peptide constructed from 12 amino acid residues derived from the N-terminal part of the neuropeptide galanin linked with a lysine residue to the 14 amino acids of the wasp venom mastoparan. Transportan can, in contrast to the galanin and mastoparan peptides alone, translocate through biological membranes and carry large hydrophilic cargos into the cell without destroying the membrane [8,9].

In a ^{1}H NMR (nuclear magnetic resonance) study of transportan in aqueous solution with sodium dodecyl sulfate (SDS) micelles, it was observed that the C-terminal mastoparan part displays α-helical secondary chemical shifts, while the galanin part is less structured. This is in agreement with what has been observed for the two peptide fragments (mastoparan and galanin) alone [10]. In order to further understand how the structures of CPPs are related to the translocating ability, a larger database of such structures is required. There are only a few examples of solution structures of CPPs in membrane mimetic solvents, mainly of penetratin, derived from the third helix of the Antennapedia transcription factor [11]. Therefore, we have determined the three-dimensional structure of transportan in a membrane-like environment, composed of phospholipid bicelles.

Bicelles are disk-shaped aggregates formed by mixing two amphiphilic molecules with different chain lengths. The size of the bicelle is controlled by changing the ratio of long-chained lipid to short-chained lipid (q). Small isotropic bicelles (with $q < 0.5$) are suitable for high-resolution NMR studies of membrane interacting peptides [12]. 1,2-Dimyristoyl-*sn*-glycero-3-phosphocholine (DMPC) is often used as the long-chained lipid, while 1,2-dihexanoyl-*sn*-glycero-3-phosphocholine (DHPC) is employed as the short-chained lipid. These zwitterionic phospholipids form stable bicelles over a relatively wide range of temperatures, concentrations, pH, and phospholipid compositions [13,14]. Phospholipid bicelles have many advantages as a membrane mimetic compared to micelles, which are commonly used in NMR investigations of membrane interacting molecules. Some enzymes (e.g., diacylglycerol kinase) that lose their biological activity in a micelle environment have been shown to maintain their function in bicelles [15]. For studies of

---

* Corresponding author. Fax: +46-8-155597.
E-mail address: lena.maler@dbb.su.se (L. Mäler).

peptide–membrane interactions, bicelles are preferred, since they resemble the surface of a membrane better than micelles [14,16]. The position of a peptide in a micelle can differ significantly from the position in a phospholipid bilayer [10,17]. Positioning studies in bicelles are therefore preferred over corresponding studies in micelles.

2. Materials and methods

2.1. Sample preparation

Transportan was obtained from Neosystem Labs and used as received. DMPC and DMPC-d$_{54}$, and DHPC and DHPC-d$_{22}$, as well as the spin-labelled lipids, 1-palmitoyl-2-steroyl-(5-DOXYL)-sn-glycero-3-phosphocholine and 1-palmitoyl-2-steroyl-(12-DOXYL)-sn-glycero-3-phosphocholine, were purchased from Avanti Polar Lipids. Samples were produced by mixing peptide and DMPC powder in phosphate buffer (50 mM, pH 5.6). A 1 M solution of DHPC-d$_{22}$ was added to produce a sample with 1 mM peptide concentration, 300 mM total lipid and $q = [\text{DMPC}]/[\text{DHPC}] = 0.33$. For NMR samples, DMPC-d$_{54}$ and DHPC-d$_{22}$ were used. 10% D$_2$O was added for field/frequency lock stabilization and 0.1 mM of 3-trimethylsilyl-propionic acid-d$_4$ (TSPA) was added as an internal reference. The sample containing transportan in dodecyl phosphocholine (DPC) was obtained by dissolving transportan in 300 mM aqueous DPC solution to yield a 1 mM peptide concentration.

2.2. Circular dichroism spectroscopy

Circular dichroism (CD) measurements were recorded for transportan in $q = 0.33$ zwitterionic bicelles and in DPC micelles, as well as in pure water. Spectra were collected on a Jasco J-720 CD spectropolarimeter using a 0.05 mm quartz cuvette. Wavelengths ranging from 190 to 250 nm were measured, with a 0.2 nm step resolution and 100 nm/min speed. The temperature was controlled by a PTC-343 controller and set to 37 °C. Spectra were collected and averaged over 16 scans. The α-helical content was estimated from the mean residue molar ellipticity at 222 nm, assuming a two-state equilibrium between α-helix and random coil conformation, $\Theta_{\alpha\text{-helix}} = -35\,700\,°\,\text{cm}^2/\text{dmol}$, and $\Theta_{RC} = 3900\,°\,\text{cm}^2/\text{dmol}$ [18].

2.3. NMR spectroscopy

NMR spectra were recorded on a Varian Inova spectrometer operating at a ^{1}H frequency of 800 MHz at 37 °C. Two-dimensional nuclear Overhauser effect spectroscopy (NOESY) [19] and total correlation spectroscopy (TOCSY) [20] spectra were typically collected as 2048×512 data point matrices using 32–64 scans. NOESY spectra were collected using two different mixing-times, 70 and 100 ms. TOCSY spectra were collected with mixing-times of 30 and 60 ms. Water-suppression was achieved with the WATERGATE method [21]. Data processing was done with FELIX (Accelrys, version 2000.1) and included zero-filling to 4096×2048 points and multiplication with a shifted sine-bell function prior to Fourier transform.

2.4. Structure calculation

551 cross-peaks in the NOESY spectrum ($\tau_{\text{mix}} = 100$ ms) recorded at 800 MHz were integrated, and the peak intensities were divided into four groups, which were given the upper distance limits 3.0, 3.5, 4.5 and 6.0 Å. This was done by normalizing the intensities against known distances as described previously [22]. In all, 220 upper distance constraints were unambiguously determined in this way and then used to calculate the structure. Structures were generated using DYANA, version 1.5, using standard annealing algorithms [23]. A total of 60 structures were calculated and a final ensemble of 25 structures was selected, based on the DYANA target function, to represent the final solution structure. No structures within the final ensemble had any distance violations larger than 0.15 Å. Analyses of the structures, including analyses of secondary structure, were performed with the PROCHECK NMR software [24] and visual analyses were performed with Insight (Accelrys, version 2000.1). Root mean square deviations (RMSDs) were calculated and overlays of structures were done with the program Suppose (http://www.scripps.edu/~jsmith/suppose). The coordinates of the final ensemble of structures together with the NMR-derived input constraints have been deposited with the Protein Data Bank (www.rcsb.org) under accession code 1SMZ.

2.5. Positioning studies

1-Palmitoyl-2-steroyl-(5-DOXYL)-sn-glycero-3-phosphocholine and 1-palmitoyl-2-steroyl-(12-DOXYL)-sn-glycero-3-phosphocholine were dissolved in methanol-d$_4$ to yield a concentration of 100 mM lipid. Spin-labelled lipids were added to the sample of transportan in bicelles to yield a concentration of 0.5 mM doxyl-labelled lipid. The effect of the spin-labels on peak heights in a 2D TOCSY spectrum ($\tau_{\text{mix}} = 30$ ms) was monitored by recording a TOCSY spectrum prior to adding the spin-labelled lipid and after addition of spin-labelled lipid. The effect of adding the doxyl-labelled lipids was evaluated from changes in amplitudes of the H^N–H$^\alpha$ cross-peaks relative to spectra without the paramagnetic probe.

3. Results

3.1. CD spectroscopy of transportan

CD spectroscopy was used to investigate the overall conformation of transportan in DPC micelles, zwitterionic bicelles and H$_2$O (Fig. 1). The measured mean molar ellipticities at 222 nm are $-11\,120\,°\,\text{cm}^2/\text{dmol}$ in bicellar solution, $-16\,230\,°\,\text{cm}^2/\text{dmol}$ in DPC and $-5860\,°\,\text{cm}^2/\text{dmol}$ in water, which gives an estimated α-helical content of 51% in DPC, 38% in the neutral bicelles and 24% in water, respectively (Fig. 1).

3.2. Solution structure of transportan in zwitterionic bicelles

Two-dimensional ^{1}H NMR spectra (TOCSY and NOESY) were recorded for 1 mM transportan in zwitterionic bicelles at 37 °C (Fig. 2) from which assignments were made. Backbone assignments were found for all residues and around 90% of the side-chain resonances could be assigned. Secondary chemical shifts for the H$^\alpha$ and H^N protons were calculated according to Wishart and Sykes [25] (Fig. 3). Both the galanin and mastoparan parts of transportan display secondary H$^\alpha$ shifts characteristic of a helical structure, and the H^N secondary shifts for the mastoparan part varies with a periodicity of three to four amino acid residues, indicative of an amphipathic helix. The structure of transportan was calculated based on 220 proton–proton distances shorter than 6 Å as determined from NOESY cross-peaks (NOEs)-derived distance constraints. The final solution structure of transportan is seen to adopt a helical
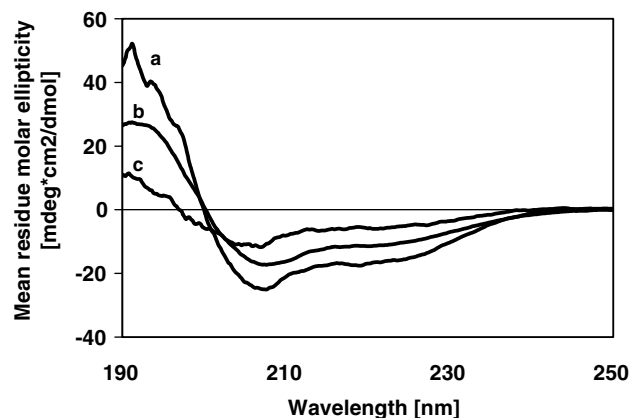

Fig. 1. CD-spectra for 1 mM transportan in DPC micelles in 50 mM phosphate buffer (a); for 1 mM transportan in neutral bicelles ([DMPC]/[DHPC] = 0.33) with 50 mM phosphate buffer, pH 5.6 (b); and for 3 mM transportan in pure H$_2$O (c). The temperature was 37 °C.
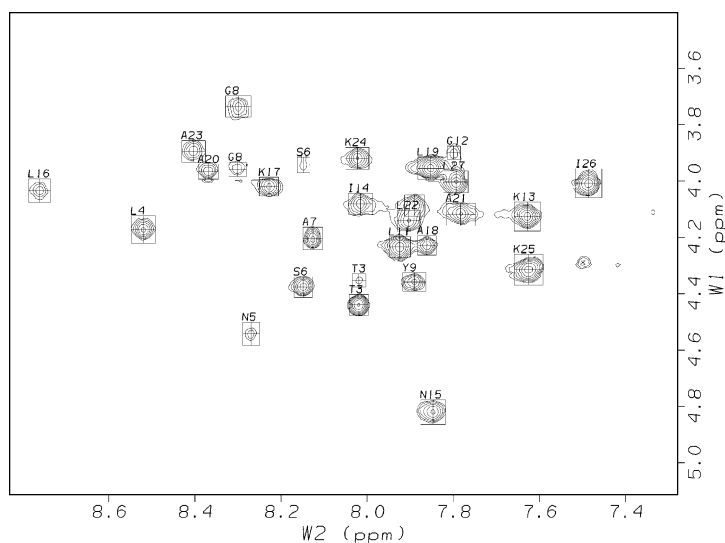
Fig. 2. The H^N–H^α fingerprint region of a TOCSY spectrum (τ_{mix} = 30 ms) recorded at 800 MHz for 1 mM transportan in neutral bicellar solution ([DMPC]/[DHPC] = 0.33) containing 50 mM phosphate buffer, pH 5.6, at 37 °C.
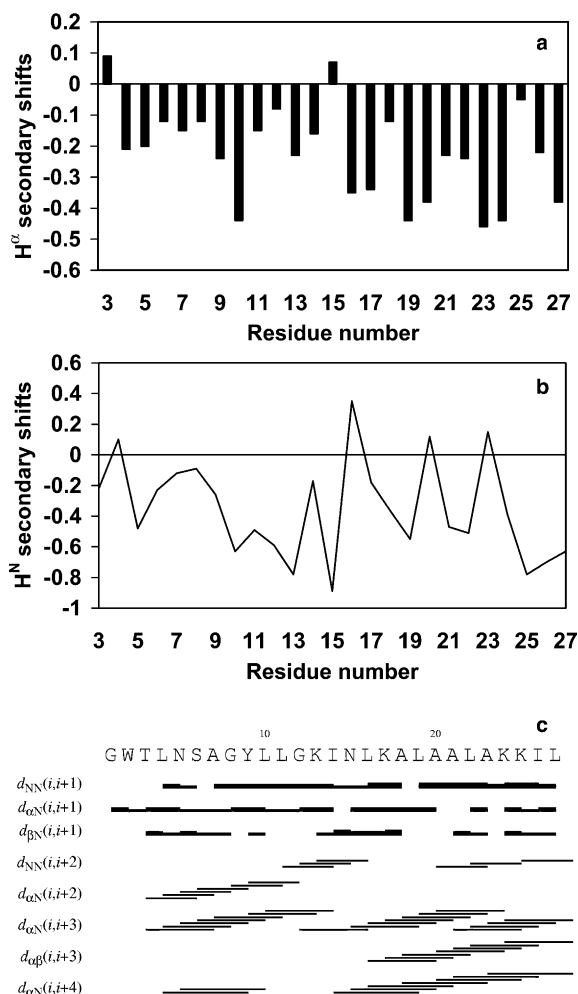

Fig. 3. Structural data for transportan in neutral bicelles. (a) H^α secondary chemical shifts. (b) H^N secondary chemical shifts. (c) Summary of sequential and medium-range NOEs obtained from the NOESY spectrum recorded with τ_{mix} = 100 ms.

conformation between residues Asn15 and Ile26 (Fig. 4). This part of the peptide has backbone torsion angles compatible with a helical structure as checked with PROCHECK NMR. A hydrogen-bonding pattern characteristic of α-helical structure is seen between residues Asn15 and Ala20. There seems to be a kink in the helix at position Ala21, since the regular NH(i)–O(i+4) hydrogen bonding pattern is interrupted by a NH(i)–O(i+3) hydrogen bond present in all structures within the ensemble. The helix becomes slightly more irregular at the C-terminal residues, since no regular hydrogen bonding pattern is observed for residues Lys24 and Lys25, but is observed for Ile26. Nevertheless, we observe a helical structure for most of the mastoparan part of the transportan peptide. The backbone RMSD in atomic coordinates for the helical part (residues 15–26) is 0.15 Å, which is significantly lower than for the whole sequence (see Table 1). The N-terminal galanin part also seems to have a weak tendency to form a helical structure, especially between residues Asn5 and Gly8 where the calculated ϕ and ψ angles fall strictly in the helical region. The number of medium range NOEs found in this part of the sequence is lower than for the C-terminus and the structure is thus much less defined (Fig. 4).

3.3. Positioning of transportan in zwitterionic bicelles

Adding the 5-doxyl- and 12-doxyl-labelled phospholipids to the peptide-bicelle solution gave similar results in terms of TOCSY H^N–H^α cross-peak broadening. The effect of the spin-labels on the TOCSY cross-peak amplitudes in the mastoparan part of the peptide is seen to oscillate with a periodicity of about three amino acids (Fig. 5). The residues most affected by the two spin-labelled phospholipids within the helix are Ala20, Ala23 and Ile26. The effect is more general on the galanin part of the peptide, but a periodicity is also seen for this part of the peptide, especially from the 12-doxyl-labelled phospholipid, affecting residues Leu4 and Ala7 significantly more than the other residues. The effect of both spin-labels is strongest for Asn15, for which the cross-peak completely vanishes, similar to what has been observed for transportan in SDS micelles [10].
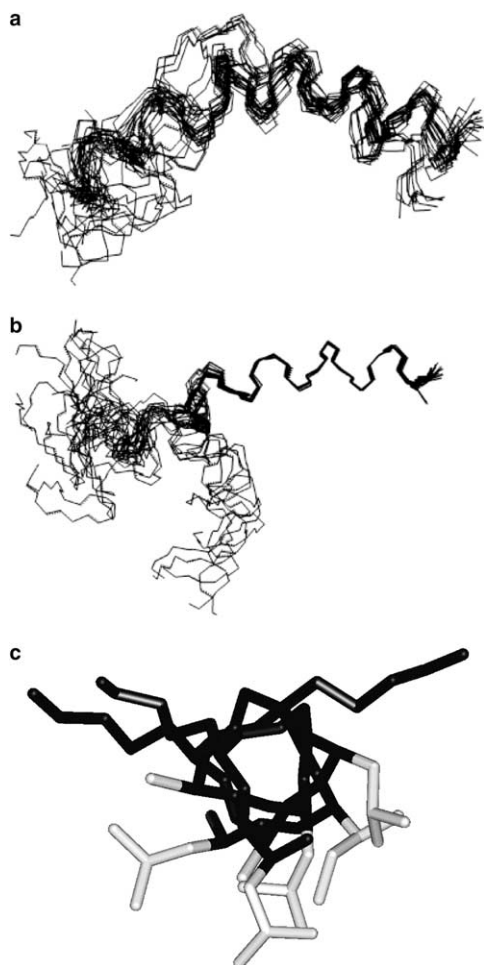
a

b

c

Fig. 4. Structure of transportan in neutral bicelles. (a,b) Overlay of the 25 structures of transportan with lowest violation energies. The structures were superimposed using backbone atoms in residues 3–26 (a) and residues 16–26 (b). (c) The C-terminal helix of transportan (residues 16–27). Leu, Ile, Ala20 and Ala23 side-chain atoms are colored in gray, and Lys side-chain atoms in black.

Table 1
Structural statistics for the ensemble of 25 transportan structures in $q = 0.33$ DMPC/DHPC bicelles calculated with DYANA

Number of constraints	220
Dyana target function	0.12 ± 0.05 Å^2
Maximum distance violation	0.13 ± 0.02 Å
Backbone atom RMSD (Å)	
All residues	2.29
Residues 3–13	0.92
Residues 15–26	0.15
Ramachandran plot regions (%)	
Most favored	79.3
Allowed region	18.1
Generously allowed	1.4
Disallowed	1.2

4. Discussion

Previous conformational analyses of transportan, based on CD measurements in vesicles with different charge densities [26], and in SDS micelles [10] show that transportan adopts a
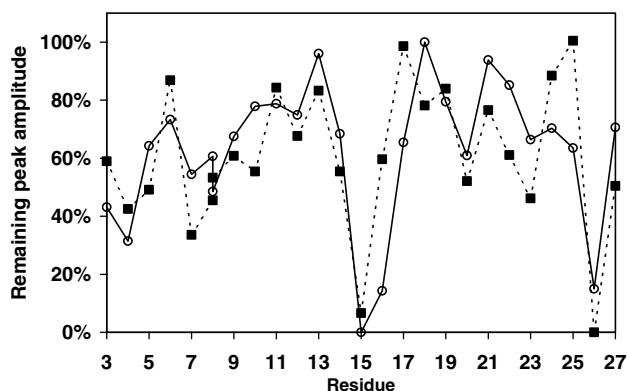

Fig. 5. The influence of 0.5 mM 1-palmitoyl-2-steroyl-(5-DOXYL)-*sn*-glycero-3-phosphocholine (solid line) and 0.5 M 1-palmitoyl-2-steroyl-(12-DOXYL)-*sn*-glycero-3-phosphocholine (dashed line) on the H^N–H$^\alpha$ cross-peaks in a TOCSY spectrum ($\tau_{mix} = 30$ ms) for transportan in neutral bicelles.

helical structure to varying degrees (40–60%). The structure changes only slightly with the properties of the membrane model system, in particular the charge density of the membrane surface. The present solution structure in small $q = 0.33$ zwitterionic bicelles suggests that the main structural feature can be derived from the helical conformation of the C-terminal mastoparan part of the chimeric peptide. This clearly indicates that the structure of the mastoparan part of the peptide is not dependent on choice of membrane model system, or on the charge density of the membrane head-group region. Structural investigations of both the galanin peptide and the mastoparan peptides have been reported previously, however, in different membrane mimetic media [12,27–29]. These studies show that mastoparan adopts a helical conformation in phospholipid bicelles, and that the galanin peptide in SDS micelles contains a series of turns, but is overall more unstructured.

The present structure in phospholipid bicelles reveals a helical conformation for the mastoparan part of transportan, and a tendency also for the galanin part of transportan to adopt a helical conformation. This is different to what was observed in the SDS study of galanin alone, and indicates a structural difference that may be partly explained by the chimera with the mastoparan peptide, and partly by the presence of the phospholipid model system. The relatively low amount of helical structure found in the CD results could be explained by an equilibrium between an unstructured form in aqueous solution and a bicelle-bound structured form. The peptide could in principle also interact with free DHPC, since it is known that an equilibrium exists between bicelle-bound and a small fraction of free DHPC [13,30].

The position of transportan relative to the bicelle surface was investigated by the addition of paramagnetic probes. The two doxyl-labelled phospholipids have approximately the same effect on the peptide. This can be explained by a high degree of lipid mobility in the membrane, resulting in a broad and overlapping distribution functions for the effect of the two doxyl-labelled phospholipids [31]. The effect of the probes indicates the presence of an amphipathic helix in the mastoparan part, with a hydrophobic side facing the interior of the bicelle. There is a remarkable agreement between the spin-label results

and the secondary H^N chemical shifts (Fig. 3(b)). Positive secondary chemical shifts are often observed for H^N protons on the more hydrophobic sides in proteins and even more so in the presence of a hydrophobic environment such as a membrane [32–34]. Conversely, negative secondary shifts may indicate interactions between the H^N protons and the more hydrophilic part of a membrane. The positive secondary shifts, which coincide with the paramagnetic broadening effect, seen for residues Leu16, Ala20 and Ala23 thus support the formation of an amphipathic helix with the hydrophobic residues facing the interior of the bilayer. The paramagnetic probes do not affect the Lys residues in the mastoparan part significantly and these residues are in the structure seen to be facing one side of the helix (Fig. 4(c)). The secondary H^N chemical shifts are similar to what has previously been found for mastoparan in phospholipid bicelles [12,27] and for transportan in SDS micelles [10]. Here, we are able to establish that the helix axis of the mastoparan part in the transportan peptide resides parallel to the membrane surface, with a hydrophobic side of the helix facing the interior.

Turning to the galanin part of transportan, we see that residues in this part are more equally affected by the spin-labels, with a slight periodicity indicating the presence of an amphipathic helix also for the N-terminus of transportan. Again, the results suggest that the hydrophobic residues face the interior of the lipid bilayer. The amphipathic character for the galanin part is, however, not as clear-cut from the H^N secondary chemical shifts. The structure is not as well defined for this part as for the mastoparan part of transportan, which supports a more random distribution of the galanin residues within the membrane bilayer. As the spin-labels are known to affect both the head-group region as well as part of the acyl chains, it is likely that the probes will significantly affect also a disordered peptide residing within this region of the bilayer [31].

It should be noted that several of the structural features reported here were also seen in the previous study in SDS; the α-helix in the mastoparan part and the peculiar hinge region between the two helices constituted mainly by Asn15. The major difference in the phospholipid bicelle solvent is the partial helix in the N-terminus, and the rather clear-cut determination of localization of the entire transportan peptide at the interface between membrane and solvent.

The amphipathic helical structure found for transportan is similar to what was previously determined for penetratin [11]. In the penetratin study, it was also found that a non-penetrating analog had a more perpendicular position in relation to the membrane than penetratin itself. The ability to form an amphipathic helical structure together with their position close to the membrane surface could therefore be of importance in providing a mechanism for CPP translocation. How this is coupled to the mechanism of translocation is a question for future work.

References

[1] Lindgren, M., Hällbrink, M., Prochiantz, A. and Langel, Ü. (2000) Trends Pharmacol. Sci. 21, 99–103.
[2] Derossi, D., Chassaing, G. and Prochiantz, A. (1998) Trends Cell Biol. 8, 84–87.
[3] Drin, G., Cottin, S., Blanc, E., Rees, A.R. and Temsamani, J. (2003) J. Biol. Chem. 278, 31192–31201.
[4] Lundberg, M. and Johansson, M. (2002) Biochem. Biophys. Res. Commun. 291, 367–371.
[5] Richard, J.P., Melikov, K., Vives, E., Ramos, C., Verbeure, B., Gait, M.J., Chernomordik, L.V. and Lebleu, B. (2003) J. Biol. Chem. 278, 585–590.
[6] Terrone, D., Sang, S.L.W., Roudaia, L. and Silvius, J.R. (2003) Biochemistry 42, 13787–13799.
[7] Sakai, N. and Matile, S. (2003) J. Am. Chem. Soc. 125, 14348–14356.
[8] Pooga, M., Hällbrink, M., Zorko, M. and Langel, U. (1998) FASEB J. 12, 67–77.
[9] Lindgren, M., Gallet, X., Soomets, U., Hällbrink, M., Bråkenhielm, E., Pooga, M., Brasseur, R. and Langel, Ü. (2000) Bioconjug. Chem. 11, 619–626.
[10] Lindberg, M., Jarvet, J., Langel, Ü. and Gräslund, A. (2001) Biochemistry 40, 3141–3149.
[11] Lindberg, M., Biverståhl, H., Gräslund, A. and Mäler, L. (2003) Eur. J. Biochem. 270, 3055–3063.
[12] Vold, R.R., Prosser, S.R. and Deese, A.J. (1997) J. Biomol. NMR 9, 329–335.
[13] Glover, K.J., Whiles, J.A., Wu, G., Yu, N.-J., Deems, R., Struppe, J.O., Stark, R.E., Komives, E.A. and Vold, R.R. (2001) Biophys. J. 81, 2163–2171.
[14] Vold, R.R. and Prosser, R.S. (1996) J. Magn. Reson. 113, 267–271.
[15] Sanders II, C.R. and Landis, G.C. (1995) Biochemistry 34, 4030–4040.
[16] Chou, J.J., Kaufman, J.D., Stahl, S.J., Wingfield, P.T. and Bax, A. (2002) J. Am. Chem. Soc. 124, 2450–2451.
[17] Lindberg, M. and Gräslund, A. (2001) FEBS Lett. 497, 39–44.
[18] Greenfield, N. and Fasman, G.D. (1969) Biochemistry 8, 4108–4116.
[19] Jeener, J., Meier, B.H., Bachmann, P. and Ernst, R.R. (1979) J. Chem. Phys. 71, 4546–4553.
[20] Braunschweiler, L. and Ernst, R.R. (1983) J. Magn. Reson. 53, 521–528.
[21] Piotto, M., Saudek, V. and Sklenár, V. (1992) J. Biomol. NMR 2, 661–665.
[22] Wüthrich, K. (1986) NMR of Proteins and Nucleic Acids. Wiley–Interscience, New York.
[23] Güntert, P., Mumenthaler, C. and Wüthrich, K. (1997) J. Mol. Biol. 273, 283–298.
[24] Laskowski, R.A., MacArthur, M.W., Moss, D.S. and Thornton, J.M. (1993) J. Appl. Crystallogr. 26, 283–291.
[25] Wishart, D.S. and Sykes, B.D. (1994) Meth. Enzymol. 239, 363–392.
[26] Magzoub, M., Kilk, K., Eriksson, G.L.E., Langel, Ü. and Gräslund, A. (2001) Biochim. Biophys. Acta 1512, 77–89.
[27] Whiles, J.A., Brasseur, R., Glover, K.J., Melacini, G., Komives, E.A. and Vold, R.R. (2001) Biophys. J. 80, 280–293.
[28] Öhman, A., Lycksell, P.-O., Juréus, A., Langel, Ü., Bartfai, T. and Gräslund, A. (1998) Biochemistry 37, 9169–9178.
[29] Hori, Y., Demura, M., Iwadate, M., Ulrich, A.S., Niidome, T., Aoyagi, H. and Asakura, T. (2001) Eur. J. Biochem. 268, 302–309.
[30] Andersson, A. and Mäler, L. (2003) FEBS Lett. 545, 139–143.
[31] Vogel, A., Scheidt, H.A. and Huster, D. (2003) Biophys. J. 85, 1691–1701.
[32] Kuntz, I.D., Kosen, P.A. and Craig, E.C. (1991) J. Am. Chem. Soc. 113, 1406–1408.
[33] Zhou, N.E., Zhu, B.-Y., Sykes, B.D. and Hodges, R.S. (1992) J. Am. Chem. Soc. 114, 4320–4326.
[34] Reymond, M.T., Huo, S., Duggan, B., Wright, P.E. and Dyson, H.J. (1997) Biochemistry 36, 5234–5244.